JOURNAL OF COMPUTATIONAL PHYSICS 85, 210–244 (1989)

# The Influence of Open Boundary Conditions on the Convergence to Steady State for the Navier–Stokes Equations

JAN NORDSTRÖM

*FFA, The Aeronautical Research Institute of Sweden, S-116 11 Bromma, Sweden**

Received June 15, 1988; revised October 3, 1988

The question of open boundary conditions of inflow and outflow type for the Navier–Stokes equations and its influence on the convergence to steady state is addressed. Both the continuous and semi-discrete problem are analysed using the energy method and the Laplace transform technique. The energy method is used to derive well-posed boundary conditions for the continuous problem. For the semi-discrete problem we use the energy method to prove that by using the well-posed boundary conditions for the continuous problem and adding a suitable numerical boundary condition well-posedness is preserved. By employing the Laplace transform technique the spectra for different types of boundary conditions are obtained. The spectra are analysed and it is shown how the choice of boundary conditions strongly affects the convergence to steady state. One-dimensional Navier-Stokes calculations are performed and the resulting convergence rates agree well with the theoretical analysis. Finally, the spectra obtained using inflow and outflow types of boundary conditions are compared with spectra obtained using periodic boundary conditions and the choice of a time-integration method for the Navier–Stokes equations is discussed. 

## 1. INTRODUCTION

A significant problem in computational fluid dynamics is how to choose boundary conditions for the Navier–Stokes equations at inflow and outflow boundaries. The most frequently used method is to use the open boundary conditions given by the Euler equations and add numerical boundary conditions of the extrapolation type, see for example [1]. This approach has both theoretical and practical disadvantages. Theoretically it means that there is not a clear separation between the boundary conditions required by the equations and the additional conditions. In practice it means that the choice of additional boundary conditions are made on a cut and trial basis.

Several authors have studied the problem, Gustafsson and Sundström [2], Oliger and Sundström [3], and Nordström [4] all used the energy method to show well-posedness of the linearised Navier–Stokes equations with constant coefficients.

* Sponsoring Agency: Swedish Board for Technical Development.



0021-9991/89 $3.00

The boundary conditions were chosen so that a basic energy estimate of the dissipative type was obtained. The dissipative type of boundary conditions derived using the energy method on the linearised problem guarantees convergence if one is sufficiently close to steady state. Dutt [5] considered the full nonlinear Navier–Stokes equations. An entropy function was used to define a norm and the energy method was used to prove boundedness of the solution. Unfortunately this approach of studying the nonlinear problem does not give any information about well-posedness, nor does it say anything about convergence to steady state. In this paper we will use the energy method on the continuous and semi-discrete constant coefficient problem to obtain criteria for well-posedness. We will also present dissipative energy estimates and boundary conditions leading to well-posedness for both the continuous and semi-discrete problem.

The energy method gives a sufficient condition for well-posedness, however, it does not provide a necessary condition. A serious limitation with the energy method is that only boundary conditions involving zero and first-order gradients can be analysed; another limitation is that no quantitative information regarding convergence rates for different boundary conditions and discretisation methods can be obtained. Recently, Engquist and Gustafsson [6] studied the influence of difference formulas and boundary conditions on the convergence rate of the Euler equations using the Laplace transform technique. Kreiss [7] used this technique to prove well-posedness for hyperbolic systems. The same technique will be used in this paper to study the influence of different boundary conditions on the convergence to steady state of the Navier–Stokes equations.

The remainder of this paper will proceed as follows. In Section 2 we discuss the relation between nonlinear, linear, and constant coefficient problems. We also relate the analysis of the homogeneous problem to the inhomogeneous one. In Section 3 we present the specific constant coefficient problem with homogeneous boundary conditions that we will analyse in the remainder of the paper. In Section 4 we use the energy method on the continuous problem to derive sufficient conditions for well-posedness, a dissipative energy estimate, and boundary conditions leading to well-posedness. In Section 5 we show how to compute the continuous and discrete spectrum of the problem and how one obtains the rate of convergence. One-dimensional Navier–Stokes computations are performed in Section 6 and the convergence rates obtained are compared with the results from the theoretical analysis. We proceed in Section 7 by investigating the problem with numerical boundary conditions. By using the energy method on the semi-discrete problem we derive sufficient conditions for well-posedness and obtain a discrete energy estimate which correspond to the continuous one obtained in Section 4. We also present one set of discrete boundary conditions leading to well-posedness. We discuss the choice of numerical time integration methods in Section 8. Finally, in Section 9 we sum up and draw conclusions.

## 2. The Initial Boundary Value Problem

Since we will analyse the Navier–Stokes equations with constant coefficients and homogeneous boundary conditions we need some basic theoretical concepts to relate that problem to the full nonlinear one. We restrict ourselves to the theory relevant for the the Navier–Stokes equations. For a more detailed discussion on these matters we refer to Kreiss and Lorenz [8] in which most of the material in this section can be found. At first we disregard the problem with boundary conditions and consider the nonlinear Cauchy problem for systems of quasi-linear partial differential equations

$$u_t = P(x, t, u, \partial/\partial x)u + F(x, t), \qquad x \in R^s, \quad 0 \leqslant t \leqslant T \tag{1}$$

with initial condition

$$u(x, 0) = f(x), \qquad x \in R^s. \tag{2}$$

The initial function $f$ and the forcing function $F$ are the data of the problem, the differential operator $P$ is assumed given. Naturally one would like problem (1), (2) to have a unique solution. Furthermore, one would like the solution to depend smoothly on the data; in other words if small perturbations are added to the data, the deviation from the unperturbed problem should be small. This leads to the concept of well-posedness. Roughly speaking, a problem is well posed if it has a unique solution and in every finite time interval it can be estimated in terms of the data. To make the concept more precise we consider the perturbed problem

$$v_t = P(x, t, v, \partial/\partial x)v + F(x, t) + \delta F(x, t), \qquad x \in R^s, \quad 0 \leqslant t \leqslant T \tag{3}$$

with initial condition

$$v(x, 0) = f(x) + \delta f(x), \qquad x \in R^s. \tag{4}$$

The following definition of well-posedness is appropriate for our purpose.

Definition 1. If the problem (1), (2) has a unique solution $u$ for $F, f$ then the nonlinear problem (1), (2) is well posed at $u$ if there is an $\varepsilon > 0$ so that for all smooth functions $\delta F$, $\delta f$ with

$$\|\delta F\| + \|\delta f\| < \varepsilon, \tag{5}$$

the perturbed problem (3), (4) is uniquely solvable and $\delta u = v - u$ satisfies

$$\|\delta u\| \leqslant K_T\{\|\delta f\| + \|\delta F\|\}. \tag{6}$$

$K_T$ may depend on $T$ but not on $\delta F$, $\delta f$.

Other definitions of well-posedness are possible, different norms can be used, and the functional form of the growth rate $K_T(T)$ can vary. Here one might add that if one wants to compute a steady state solution (which is our main interest), $K_T$ has to decrease with time.

Obviously the definition of well-posedness for the nonlinear problem is closely related to well-posedness of the linearised problem. Roughly speaking the following linearisation principle holds: *A nonlinear problem is well posed at u if the linear problems obtained by linearizing at all functions near u are well posed.* Thus we have related well-posedness of the nonlinear problem to well-posedness of a set of linearised problems. It is desirable to relate linear problems to constant coefficient problems. This can be done using the following localisation principle: *If all constant coefficient problems are well posed and the solution can be estimated in terms of the initial function itself (no gradients of the initial function are allowed in the estimate) then the corresponding variable coefficient problem is also well posed.* It should be observed that the localisation principle is not valid for general linear variable coefficient operators, but fortunately it is valid for those operators that appear in the context of the Navier–Stokes equations, namely: hyperbolic, parabolic, and operators of mixed hyperbolic–parabolic type. For proofs and more details concerning these principles see Kreiss and Lorenz [8].

Now we will relate the homogeneous initial boundary value problem to the inhomogeneous one. Consider a linear system of differential equations,

$$u_t = P(x, t, \partial/\partial x)u + F(x, t), \qquad x \in \Omega, \quad t \geqslant 0 \tag{7}$$

$$u(x, 0) = f(x) \qquad x \in \Omega \tag{8}$$

$$Lu = g(x, t) \qquad x \in \partial\Omega. \tag{9}$$

$L$ is a linear operator combining values of $u$ and its gradients on the boundary $\Gamma = \partial\Omega$. We consider $F$, $f$, and $g$ as the data of the problem. The operators $P$, $L$ and the domain $\Omega$ are fixed. We now define well-posedness for the problem (7), (8), and (9).

DEFINITION 2. The initial boundary value problem (7), (8), (9) is well-posed if for all smooth compatible data $F$, $f$, $g$ there is a unique solution $u$, and for every finite time interval $0 \leqslant t \leqslant T$ there is a constant $K_T$ such that

$$\|u(\cdot, t)\|^2 + \int_0^t \|u(\cdot, \xi)\|_\Gamma^2 \, d\xi \leqslant K_T \left\{ \|f\|^2 + \int_0^t \|F(\cdot, \xi)\|^2 \, d\xi + \int_0^t \|g(\cdot, \xi)\|_\Gamma^2 \, d\xi \right\}. \tag{10}$$

The constant $K_T$ does not depend on $F$, $f$, or $g$ but may depend on $T$.

Naturally it would be nice if it was sufficient to analyse the problem with zero data. Using Duhamel's principle (see [8]) one can show that the forcing function

$F$ is of no importance for well-posedness; in other words if the problem is well posed for $F=0$ it is also well posed for $F\neq 0$ and one just adds

$$\int_0^t \|F(\cdot, \xi)\|^2 \, d\xi \tag{11}$$

to the right-hand side of the estimate. Let us see what the effect of homogeneous initial conditions has on the estimate (10). By introducing the variable $v(x, t)=u(x, t)-\exp(-t)f(x)$, we obtain zero initial data for $v$. The corresponding differential equation becomes

$$v_t = Pv + F + \exp(-t)\{f + Pf\}. \tag{12}$$

Therefore using (10) we can estimate $v$ in terms of the new forcing function $G=F+\exp(-t)\{f+Pf\}$. The resulting estimate for $u$ is the same as (10) with $F$ replaced by $G$. Unfortunately, it involves gradients of $f$ and is therefore not of the same type. If $Pf$ is singular at $t=0$, we might have problems. Now what about homogeneous boundary conditions? We make the transformation $v(x, t)=u(x, t)-\phi(x)\,g(t)$, where $\phi$ is chosen so that $v$ has zero boundary data. Furthermore, we choose $\phi$ to be a smooth function that decays to zero away from the boundary $\Gamma$. The differential equation for $v$ becomes

$$v_t = Pv + F + gP\phi - \phi g_t. \tag{13}$$

By once more using (10) we can estimate $v$ and therefore also $u$. The forcing function in this case is $F+gP\phi-\phi g_t$. This time we get an additional term involving time derivatives of $g$ on the right-hand side of (10).

## 3. The Navier–Stokes Equations

We consider the linearised and symmetrised Navier–Stokes equations in two space dimensions with initial conditions and homogeneous boundary conditions:

$$\begin{aligned} q_t + Aq_x + Bq_y + \varepsilon\{Cq_{xx} + Eq_{xy} + Dq_{yy}\} &= 0, \qquad (x, y)\in\Omega, \quad t\geqslant 0 \\ q(x, y, 0) - f(x, y) &= 0, \qquad (x, y)\in\Omega \\ A_0 q(0, y, t) + B_0 q_x(0, y, t) + C_0 q_{xx}(0, y, t) &= 0 \\ A_1 q(1, y, t) + B_1 q_x(1, y, t) + C_1 q_{xx}(1, y, t) &= 0 \end{aligned} \tag{14}$$

The Navier–Stokes equations are linearised around a constant state $\bar{Q}=(\bar{\rho}, \bar{u}, \bar{v}, \bar{T})^{\mathrm{T}}$ and symmetrised using the "parabolic" symmetriser derived by Abarbanel and Gottlieb [9], see also Nordström [10]. The perturbation $q$ is defined by $q=\Lambda Q$, where $\Lambda=\mathrm{diag}(\bar{c}/\bar{\rho}, \sqrt{\gamma}, \sqrt{\gamma}, \gamma\sqrt{(\gamma-1)}/\bar{c})$. $A$, $B$, $C$, $D$, and $E$ are four by four constant symmetric matrices listed in the Appendix. The domain $\Omega$ is the strip

$(x, y) \in [0, 1] \times [-\infty, +\infty]$. The matrices $A_0, B_0, C_0, A_1, B_1$, and $C_1$ express boundary conditions on the inflow and outflow boundaries and will be specified later. We include second-order derivatives in the boundary conditions for reasons that will become obvious later when we compare the discrete spectrum with the continuous one.

The dependent variables and parameters $\rho$, $u$, $v$, $T$, $p$, $c$, $M$, $\mu$, $\lambda$, $k$, Pr, $\gamma$, Re, and $\varepsilon$ are respectively the density, $x$ and $y$ components of the velocity, the temperature, the pressure, the speed of sound, the Mach number, the shear and second viscosity, the coefficient of heat conduction, the Prandtl number, the ratio of specific heats, the Reynolds number, and the inverse Reynolds number. All variables are non-dimensionalised with reference quantities. We use an overbar to denote a variable with a constant state unless it is obvious. In most of this investigation we consider a uniform flow and we use the following numerical values on the variables unless otherwise stated.

$$\begin{aligned} &\bar{\rho} = 1, \quad \bar{u} = 1 \qquad \bar{v} = 0, \quad \bar{T} = 1/(\gamma(\gamma - 1)\, M^2), \quad \bar{c} = 1/M \\ &\bar{\mu} = 1, \quad \bar{\lambda} = -2/3, \quad \bar{k} = 1, \quad \mathrm{Pr} = 0.7, \qquad\qquad \gamma = 1.4. \end{aligned} \tag{15}$$

In the $y$-direction we have no boundaries and therefore we Fourier-transform (14) with respect to that variable:

$$\begin{aligned} \phi_t + U^{(0)}\phi + U^{(1)}\phi_x + U^{(2)}\phi_{xx} &= 0, \qquad x \in [0, 1],\ t \geqslant 0 \\ \phi(x, \omega, 0) - \hat{f}(x, \omega) &= 0, \qquad x \in [0, 1] \\ A_0\phi(0, \omega, t) + B_0\phi_x(0, \omega, t) + C_0\phi_{xx}(0, \omega, t) &= 0, \\ A_1\phi(1, \omega, t) + B_1\phi_x(1, \omega, t) + C_1\phi_{xx}(1, \omega, t) &= 0. \end{aligned} \tag{16}$$

The Fourier transformed variable $q$ is denoted by $\phi$; this notation will be kept for the rest of the paper. The matrices $U^{(0)}$, $U^{(1)}$, and $U^{(2)}$ are functions of the Mach number, the Reynolds number, and the wave number $\omega$ in the $y$ direction:

$$\begin{aligned} U^{(0)} &= i\omega B(M) + (i\omega)^2 \varepsilon D \\ U^{(1)} &= A(M) + i\omega\varepsilon E \\ U^{(2)} &= \varepsilon C. \end{aligned} \tag{17}$$

Later on we will use the Laplace transform to compute the spectrum of the problem. The Laplace transformed version of (16) is

$$\begin{aligned} (U^{(0)} + sI)\varphi + U^{(1)}\varphi_x + U^{(2)}\varphi_{xx} &= \hat{f}(x, \omega), \qquad x \in [0, 1] \\ A_0\varphi(0, \omega, s) + B_0\varphi_x(0, \omega, s) + C_0\varphi_{xx}(0, \omega, s) &= 0 \\ A_1\varphi(1, \omega, s) + B_1\varphi_x(1, \omega, s) + C_1\varphi_{xx}(1, \omega, s) &= 0. \end{aligned} \tag{18}$$

The Laplace and Fourier transformed vector $q$ is denoted by $\varphi$, this notation will

be kept for the rest of the paper. The Laplace transformation will formally be justified in Section 4 below. For later reference we also introduce the inner product and norms for the continuous problem:

$$\|\hat{q}\|^2 = \|\phi(\cdot, \omega, t)\|^2 = \int_0^1 \phi^* \phi \, dx$$

$$\|q\|^2 = \int_{-\infty}^{+\infty} \|\phi\|^2 \, d\omega = \int_{-\infty}^{+\infty} \int_0^1 q^* q \, dx \, dy \tag{19}$$

$$\phi^* \phi = \sum_{i=1}^{4} \bar{\phi}_i \phi_i.$$

In (19) the overbar denotes a complex conjugated quantity.

## 4. The Energy Method

To derive boundary conditions we use the energy method. We state the basic result from which the boundary conditions are derived.

THEOREM 1. *If the boundary conditions in* (14) *are such that the conditions*

$$\begin{aligned} [q^T A q + 2\varepsilon q^T C q_x]_{x=0} &\leqslant 0 \\ [q^T A q + 2\varepsilon q^T C q_x]_{x=1} &\geqslant 0 \end{aligned} \tag{20}$$

*are satisfied, then the problem is well posed and q satisfies the estimate*

$$\|q\|^2 + \varepsilon\alpha \int_0^t \{\|q_x^{(2)}\|^2 + \|q_y^{(2)}\|^2\} \, d\tau \leqslant \|f\|^2. \tag{21}$$

*We have used the notation* $q^{(2)} = (q_2, q_3, q_4)^T$ *and* $\alpha$ *is a positive constant of order one.*

It should be mentioned here that the estimate (21) can be sharpened even more by including the time integral of $|q|^2$ at the boundaries on the left-hand side of the inequality.

*Proof.* Using Eq. (16), multiplying with the complex conjugated transpose of $\phi$, and integrating with respect to $x$ we obtain

$$(\|\phi\|^2)_t - \varepsilon \int_0^1 \begin{pmatrix} \phi i\omega \\ \phi_x \end{pmatrix}^* \Psi \begin{pmatrix} \phi i\omega \\ \phi_x \end{pmatrix} dx = -[\phi^* A \phi + \varepsilon(\phi^* C \phi_x + \phi_x^* C \phi)]_0^1, \tag{22}$$

where

$$\Psi = \begin{pmatrix} 2D & E \\ E & 2C \end{pmatrix}. \tag{23}$$

The matrix $\Psi$ is Hermitian and has nonpositive eigenvalues; the eigenvalues are

$$\begin{aligned}\lambda_{1,2} &= 0\\ \lambda_{3,4} &= -2(\gamma\bar{k}/\mathrm{Pr})/\bar{\rho}\\ \lambda_{5,6} &= -2\bar{\mu}/\bar{\rho} \pm (\bar{\lambda}+\bar{\mu})/\bar{\rho}\\ \lambda_{7,8} &= -2(\bar{\lambda}+2\bar{\mu})/\bar{\rho} \pm (\bar{\lambda}+\bar{\mu})/\bar{\rho}.\end{aligned} \tag{24}$$

By using Parseval's relation on (22), condition (20), and an estimate of the matrix $\Psi$, we get

$$(\|q\|^2)_t + \varepsilon\alpha\{\|q_x^{(2)}\|^2 + \|q_y^{(2)}\|^2\} \leqslant 0. \tag{25}$$

The estimate (21) is obtained by integration. Uniqueness follows directly from the energy estimate (21). Assume that we have another solution $\bar{q}$ satisfying the same equation with the same initial and boundary conditions, then, since the problem is linear, $\xi = q - \bar{q}$ is also a solution but with zero initial condition. Using Eq. (21) we get $\xi \equiv 0$. We will now proceed to show estimates for all higher $x$-derivatives of $\phi$. By differentiating (16) we see that $\phi_t$ satisfies the same differential equation as $\phi$ with the same boundary conditions. This implies

$$\|\phi_t\| \leqslant \|\phi_t(0)\| = \|U^{(0)}\hat{f} + U^{(1)}\hat{f}_x + U^{(2)}\hat{f}_{xx}\|. \tag{26}$$

We get the estimate

$$\|\phi_t\| = \text{const}\left\{\sum_{n=0}^{2} \|d^n\hat{f}/dx^n\|\right\}. \tag{27}$$

To show estimates for the $x$-derivatives we partition $\phi$ and the matrices $U^{(0)}$, $U^{(1)}$, and $U^{(2)}$ into blocks. The partitioned form of (16) is

$$\phi_t^{(1)} = -U_{11}^{(0)}\phi^{(1)} - U_{12}^{(0)}\phi^{(2)} - U_{11}^{(1)}\phi_x^{(1)} - U_{12}^{(1)}\phi_x^{(2)} \tag{28}$$

$$\phi_t^{(2)} = -U_{21}^{(0)}\phi^{(1)} - U_{22}^{(0)}\phi^{(2)} - U_{21}^{(1)}\phi_x^{(1)} - U_{22}^{(1)}\phi_x^{(2)} - U_{22}^{(2)}\phi_{xx}^{(2)}. \tag{29}$$

Since $U_{11}^{(1)} = \bar{u}$ is nonsingular we can express $\phi_x^{(1)}$ in terms of $\phi$, $\phi_t$, and $\phi_x^{(2)}$ by using the first equation. The second equation gives us

$$\|\phi_{xx}^{(2)}\| \leqslant \text{const}\left\{\sum_{n=0}^{2} \|d^n\hat{f}/dx^n\|\right\}. \tag{30}$$

Now we have estimates for $\phi$, $\phi_t$, $\phi_x$, and $\phi_{xx}^{(2)}$, repeated differentiation and application of the same technique will give us estimates of all $x$-derivatives as long as the initial data can be differentiated. By using Parseval's theorem we get the corresponding estimates for the untransformed variables. By using the Sobolev inequality

$$|q|_\infty^2 \leqslant 2\{\|q\|^2 + \|q_x\|^2\}, \tag{31}$$

we can bound all $x$-derivatives in the maximum norm. To conclude the proof of the theorem we must show existence. This can be done using the Laplace transform technique. The Laplace transformation is justified since all gradients of $q$ are bounded and we can formally obtain a solution in the way that will be described in Section 5 below. This concludes the proof.

As can be seen in (20) the wave number $\omega$ does not influence well-posedness; what about the influence of $\omega$ on the total dissipation? In Fig. 1 the decay rates (a measure of the total dissipation, see Section 5) for a set of boundary conditions (denoted below by B.C.1) giving a well-posed problem are plotted for three different Reynolds numbers. One clearly see that the total dissipation has a minimum for $\omega \neq 0$ and consequently the least dissipative case is not 1-dimensional.

To derive explicit boundary conditions we will use condition (20). The quadratic form in (20) can be written

$$\begin{aligned} q^{\mathrm{T}}Aq + 2\varepsilon q^{\mathrm{T}}Cq_x = &+ \{(\bar{u}-\bar{c})\,\bar{c}^2/2\gamma\bar{p}^2\}[p-\bar{\rho}\bar{c}u]^2 \\ &+ \{\bar{u}\bar{c}^2/\gamma(\gamma-1)\,\bar{p}^2\}[p-\rho\bar{c}^2]^2 \\ &+ \{\gamma\bar{u}\}[v]^2 \\ &+ \{(\bar{u}+\bar{c})\,\bar{c}^2/2\gamma\bar{p}^2\}[p+\bar{\rho}\bar{c}u]^2 \\ &- \{2\gamma\varepsilon/\bar{\rho}\}[(\bar{\lambda}+2\bar{\mu})\,uu_x + \bar{\mu}vv_x + (\gamma\bar{k}/Pr)\,TT_x/\bar{T}]. \end{aligned} \tag{32}$$

At $x=0$ we have inflow and at $x=1$ we have outflow (the velocity $\bar{u}$ is always

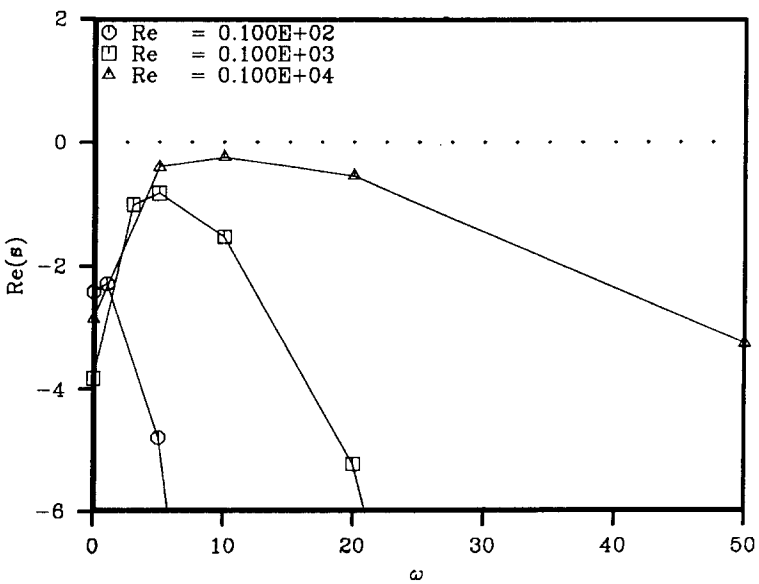


FIG. 1. Decay rates for B.C.1, Ma = 0.5.

positive). When constructing boundary conditions for the Navier–Stokes equations it is suitable to choose boundary conditions so that the Euler equations are well posed and then augment these using the right number of derivative boundary conditions so that the gradient terms within the brackets of (32) have the right sign. Since we derive boundary conditions for the linearised problem, the boundary conditions for the nonlinear problem are obtained by integrating the homogeneous boundary conditions for the linearised problem. To get useful boundary conditions for the full nonlinear problem we therefore demand that the boundary conditions for the linear problem form total differentials.

The number of boundary conditions for the Navier–Stokes equations is obtained by considering the mathematical structure of the equations. It consists of a hyperbolic scalar equation (the continuity equation) and a parabolic set of equations (in two dimensions we have two momentum equations and one energy equation). For the parabolic part of the equations we have to pose three boundary conditions at any type of boundary. In the hyperbolic case we have to specify one boundary condition if the characteristic variable $\rho$ propagates into the domain otherwise not. For the Navier–Stokes equations in two dimensions this means that we have to give four boundary conditions at an inflow boundary and three at an outflow boundary. For more details on how to determine the number of boundary conditions see Strikwerda [11].

*Supersonic inflow*, $x=0$, $\bar{u}>\bar{c}$. We should give four boundary conditions both for the Euler and Navier–Stokes equations. The coefficients in front of the squared brackets in (32) are all positive which means we have to set all variables to zero:

$$\rho=0, \qquad u=0, \qquad v=0, \qquad T=0. \tag{33}$$

*Subsonic inflow*, $x=0$, $\bar{u}<\bar{c}$. Three boundary conditions should be given for the Euler equations and four for the Navier–Stokes equations. Three of the coefficients multiplying the squared brackets are positive, the fourth boundary condition is used to make the gradient terms zero:

$$\begin{aligned} u+2c(\gamma-1)^{-1}&=0, \qquad & T\bar{T}^{-1}-(\gamma-1)\,\rho\bar{\rho}^{-1}&=0\\ v&=0, \qquad & (\lambda+2\mu)\,u_x-2(k/\mathrm{Pr})\,c_x&=0. \end{aligned} \tag{34}$$

*Supersonic outflow*. $x=1$, $\bar{u}>\bar{c}$. Three boundary conditions should be given for the Navier–Stokes equations and none for the Euler equations. None of the coefficients are positive; the three boundary conditions are all used to set the gradient terms to zero:

$$u_x=0, \qquad v_x=0, \qquad T_x=0. \tag{35}$$

*Subsonic outflow*, $x=1$, $\bar{u}<\bar{c}$. One boundary condition should be applied for

the Euler equations and three for the Navier–Stokes equations. One coefficient is positive, the two additional conditions are used to set the gradient terms to zero:

$$u \text{ or } p-\varepsilon(\lambda+2\mu)\,u_x=0, \qquad v_x=0, \qquad T_x=0. \tag{36}$$

We can summarise the results in the following theorem.

THEOREM 2. *If the boundary conditions in* (14) *are given by* (33) *at a supersonic inflow boundary,* (34) *at a subsonic inflow boundary,* (35) *at a supersonic inflow boundary, and* (36) *at a subsonic outflow boundary then the problem is well posed and the solution q satisfies the estimate* (21).

The boundary conditions (33), (34), (35), and (36) were obtained by Gustafsson and Sundström [2] while the subsonic outflow boundary condition $p-\varepsilon(\lambda+2\mu)\,u_x=0$ was obtained by Nordström [4]. The characteristic boundary conditions used for the Eular equations are obtained from (32) by setting the terms within the squared brackets to zero when the sign of the corresponding coefficient so indicates and ignore the gradient terms.

## 5. THE SPECTRUM

The Laplace transform is defined by

$$\tilde{u}(s)=Lu=\int_0^\infty u\exp(-st)\,dt. \tag{37}$$

The transformation (37) can be done if $\Re(s)$ is large enough and $u$ has at most exponential growth ($\Re(s)$ denotes the real part of $s$). Formally the transformation of (16) was justified in Section 4 above where it was shown that we can estimate all $x$-derivatives of $\phi$. By applying the Laplace transform to (16) we got (18) which is a system of ordinary differetial equations with constant coefficients. We assume an exponential behaviour of the homogeneous part of the solution. By inserting $\varphi=\psi\exp(\kappa x)$ into (18) we obtain

$$\{U^{(2)}\kappa^2+U^{(1)}\kappa+(U^{(0)}+sI)\}\psi=0. \tag{38}$$

Equation (38) has a non-trivial solution if and only if:

$$|U^{(2)}\kappa^2+U^{(1)}\kappa+(U^{(0)}+sI)|=0. \tag{39}$$

From Eq. (38) and (39) we can solve for $\kappa$ and $\psi$ as functions of $s$. The homogeneous solution can formally be written:

$$\varphi_h=\sum_{i=1}^{7}\sigma_i\psi^i(s)\exp(\kappa_i(s)x). \tag{40}$$

The form (40) of the solution is not valid for multiple eigenvalues $\kappa(s)$. In that case we would assume that the eigenvector $\psi$ is an $n$th degree polynomial in $x$ where $n+1$ is the multiplicity of the eigenvalue $\kappa(s)$. We do not consider this case theoretically but in the computations discussed below it is always checked that no multiple eigenvalues are present. The particular solution $\varphi_p$ which depends on the initial function $\hat{f}$ is (as will become obvious later) of no interest to us; we simply assume that it is known. The coefficients in (40) are determined by the boundary conditions which give us the following equation for $\sigma = (\sigma_1, \sigma_2, ..., \sigma_7)^T$.

$$E(s)\sigma = -H. \tag{41}$$

$E(s)$ is a seven by seven matrix (four inflow conditions and three outflow conditions). $H$ depends on the particular solution and its derivatives on the boundaries. To get a unique solution of (41) we must choose $s$ so that $\Re(s) > \Re(s^*)$, where

$$\Re(s^*) = \max_s \Re(s) \qquad \forall s \in \{s; |E(s)| = 0\}. \tag{42}$$

If $\Re(s) > \Re(s^*)$ we can solve for $\sigma$ and finally get the solution by taking the inverse Laplace transform to get $\phi$:

$$\phi = L^{-1}\varphi = \exp(\Re(s^*)t)\left\{\frac{1}{2\pi i}\int_{-i\infty}^{+i\infty} \varphi(s + \Re(s^*))\exp(st)\,ds\right\}. \tag{43}$$

For convergence to steady state it is essential that $\Re(s^*)$ is strictly less than zero; otherwise the solution grows exponentially with time. For obvious reasons we hereafter denote $\Re(s^*)$ with the decay rate (D.R.($C$)) of the continuous problem. The distribution of singular values of $\varphi$, the continuous spectrum, is given by solving

$$|E(s)| = 0 \tag{44}$$

for $s$. Due to the complexity of Eqs. (38), (39), and (44) we have to use numerical methods to obtain the continuous spectrum. First the determinant in (39) is expanded into a seventh degree polynomial in $\kappa$ and a standard library routine is used to compute $\kappa_i(s)$ for $i = 1, 2, ..., 7$. Second, the corresponding eigenvectors $\psi_i(\kappa_i(s), s)$ are computed using (38). Now we have the eigenvectors $\psi_i$ and the eigenvectors $\psi_i(\kappa_i(s), s)$ are computed using (38). Now we have the eigenvectors $\psi_i$ and the eigenvalues $\kappa_i$ as functions of $s$ and with given boundary conditions we can construct the matrix $E(s)$ and therefore also $|E(s)|$. Equation (44) is solved using the secant method.

Now we turn to the semi-discrete problem. We discretised the problem (16) by using the centered finite volume method:

$$
\begin{aligned}
(\phi_i)_t &= A_i^L \phi_{i-1} + A_i^M \phi_i + A_i^R \phi_{i+1}, \qquad && i = 1, 2, ..., N \\
\phi_i(0) &= \hat{f}_i && i = 0, 1, ..., N+1 \\
\phi_0 &= B_0 \phi_1 + C_0 \phi_2 \\
\phi_{N+1} &= B_N \phi_N + C_N \phi_{N-1}.
\end{aligned} \tag{45}
$$

The function values $\phi_i = \phi((x_i + x_{i+1})/2, \omega, t)$ are located in the middle of the cell and the value of $\phi$ at a cell boundary $x_i$ is given by $(\phi_i + \phi_{i-1})/2$. The gridpoints $x_0$ and $x_{N+1}$ are located just outside of the boundaries. The matrices involved are functions of $\Delta x_i = x_{i+1} - x_i$:

$$
\begin{aligned}
A_i^L &= +U^{(1)}\left(\frac{1}{2\Delta x_i}\right) - 2U^{(2)}\left(\frac{1}{(\Delta x_{i-1} + \Delta x_i)\,\Delta x_i}\right) \\
A_i^M &= -U^{(0)} + U^{(2)}\left(\frac{2}{(\Delta x_{i-1} + \Delta x_i)\,\Delta x_i} + \frac{2}{(\Delta x_{i+1} + \Delta x_i)\,\Delta x_i}\right) \\
A_i^R &= -U^{(1)}\left(\frac{1}{2\Delta x_i}\right) - 2U^{(2)}\left(\frac{1}{(\Delta x_{i+1} + \Delta x_i)\,\Delta x_i}\right).
\end{aligned} \tag{46}
$$

For the boundary points we get the equations

$$
\begin{aligned}
(\phi_1)_t &= A_1'^M \phi_1 + A_1'^R \phi_2 \\
(\phi_N)_t &= A_N'^M \phi_N + A_N'^L \phi_{N-1},
\end{aligned} \tag{47}
$$

where

$$
\begin{aligned}
A_1'^M &= A_1^M + A_1^L B_0, \qquad & A_1'^R &= A_1^R + A_1^L C_0 \\
A_N'^M &= A_N^M + A_N^R B_N, \qquad & A_N'^L &= A_N^L + A_N^R C_N.
\end{aligned} \tag{48}
$$

We can now write the system (45) in a more compact form,

$$
\begin{aligned}
\boldsymbol{\phi}_t &= \mathbf{A}\boldsymbol{\phi} \\
\boldsymbol{\phi}(0) &= \mathbf{f},
\end{aligned} \tag{49}
$$

where

$$
\begin{aligned}
\boldsymbol{\phi} &= (\phi_1, \phi_2, ..., \phi_{N-1}, \phi_N)^{\mathrm{T}} \\
\mathbf{f} &= (\hat{f}_1, \hat{f}_2, ..., \hat{f}_{N-1}, \hat{f}_N)^{\mathrm{T}}
\end{aligned} \tag{50}
$$

$$
\mathbf{A} = \begin{pmatrix}
A_1'^M & A_1'^R & \cdots & \cdots & \cdots & 0 \\
A_2^L & A_2^M & A_2^R & & & \vdots \\
\vdots & \ddots & \ddots & \ddots & & \vdots \\
\vdots & & \ddots & \ddots & \ddots & \vdots \\
\vdots & & & A_{N-1}^L & A_{N-1}^M & A_{N-1}^R \\
0 & \cdots & \cdots & \cdots & A_N'^L & A_N'^M
\end{pmatrix}. \tag{51}
$$

Now we Laplace-transform Eq. (49) and obtain

$$(\mathbf{A} - sI)\boldsymbol{\varphi} = -\mathbf{f}. \tag{52}$$

Similarly to the continuous problem we must choose $s$ so that $\Re(s) > \Re(s^*)$, where $s^*$ is the eigenvalue of $\mathbf{A}$ with the largest real part. If $\Re(s) > \Re(s^*)$ we can solve for $\boldsymbol{\varphi}$ in (52) and finally find the solution by taking the inverse Laplace transform to obtain $\boldsymbol{\phi}$:

$$\boldsymbol{\phi} = L^{-1}\boldsymbol{\varphi} = \exp(\Re(s^*)t)\left\{\frac{1}{2\pi i}\int_{-i\infty}^{+i\infty} \boldsymbol{\varphi}(s + \Re(s^*))\exp(st)\,ds\right\}. \tag{53}$$

Just as in the continuous case, it is essential for convergence to steady state that $\Re(s^*)$, the discrete decay rate (D.R.($D$)), is strictly less than zero. The distribution of singular values of $\boldsymbol{\varphi}$, the discrete spectrum, is given by solving

$$|\mathbf{A} - sI| = 0 \tag{54}$$

for $s$.

To verify the codes we shall compare the continuous and discrete spectra, but first we have some comments on how to simulate numerical boundary conditions in the continuous case. Consider for simplicity a uniform mesh; assume that $h(x - \Delta x)$ and $h(x)$ are known. If we use zero or first-order extrapolation to obtain $h(x + \Delta x)$, it corresponds to setting the first or second derivative to zero, since

$$\begin{aligned} h(x)_x &= \{h(x + \Delta x) - h(x)\}/\Delta x + O(\Delta x) \\ h(x)_{xx} &= \{h(x + \Delta x) - 2h(x) + h(x - \Delta x)\}/2\Delta x + O(\Delta x^2). \end{aligned} \tag{55}$$

We will investigate three types of continuous boundary conditions and restrict ourselves to subsonic flow.

B.C.1, 4. These boundary conditions are derived using the energy method. One can choose to extrapolate $\rho$ or $u$ to get the numerical boundary condition (denoted by **). If $\rho$ is chosen, the discrete boundary condition is denoted B.C.1; if we extrapolate $u$, we denote that B.C.4:

| Inflow boundary | Outflow boundary | |
|---|---|---|
| $u + 2c/(\gamma - 1) = 0$ | $p - \varepsilon(\lambda + 2\mu)u_x = 0$ | |
| $T/\bar{T} - (\gamma - 1)\rho/\bar{\rho} = 0$ | $v_x = 0$ | |
| $v = 0$ | $T_x = 0$ | |
| $(\lambda + 2\mu)u_x - (2(k/\mathrm{Pr})c_x = 0$ | $\rho_{xx}$ or $u_{xx} = 0$ | ** |

(56)

B.C.2. It is common in Euler calculations to specify $\rho$, $u$, and $v$ at the inflow boundary and $p$ at the outflow boundary; the numerical boundary conditions are

found by extrapolation. In Navier–Stokes calculation this procedure is also often used. As we have seen, one should give four inflow conditions and three outflow conditions for the continuous Navier–Stokes equations. For the sake of comparison we therefore have to simulate one inflow condition and two outflow conditions. We simulate zero and first-order extrapolation by setting the first and second derivative to zero, respectively, see (55). The simulated continuous boundary conditions are denoted by $*$, while as was mentioned above $**$ is used to indicate a numerical boundary condition:

| Inflow boundary | Outflow boundary |
|---|---|
| $\rho = 0$ | $p = 0$ |
| $u = 0$ | $u_{xx} = 0$ $*$ |
| $v = 0$ | $v_{xx} = 0$ $*$ |
| $T_x = 0$ $*$ | $\rho_{xx} = 0$ $**$ |

(57)

B.C.3. Another common set of boundary conditions for the Euler equations is found by specifying the ingoing characteristics and extrapolating the outgoing ones. The same procedure is common in Navier–Stokes computations. The notations are the same as discussed above:

| Inflow boundary | Outflow boundary |
|---|---|
| $(p - \bar{\rho}\bar{c}u)_{xx} = 0$ $*$ | $p - \bar{\rho}\bar{c}u = 0$ |
| $p - \rho\bar{c}^2 = 0$ | $(p - \rho\bar{c}^2)_{xx} = 0$ $*$ |
| $v = 0$ | $v_{xx} = 0$ $*$ |
| $p + \bar{\rho}\bar{c}u = 0$ | $(p + \bar{\rho}\bar{c}u)_{xx} = 0$ $**$ |

(58)

Now we will compare the continuous spectrum with the discrete one. The continuous spectrum has an infinite number of eigenvalues $s$ while the discrete spectrum has $4N$ eigenvalues, since $q$ has four components and $N$ is the number of gridpoints. For fixed values of the parameters involved we should expect convergence of the discrete spectrum to the continuous one for $N \to \infty$. Furthermore, with a given number of gridpoints we can only expect to resolve the eigenvalues corresponding to the smoothest eigensolutions and, consequently, parts of the discrete spectrum will have no similarity with the continuous spectrum. It is, however, essential that the eigenvalue located to the utmost right in the complex plane is well predicted since that eigenvalue determines the decay rate.

Before discussing the results from the computations we give some remarks about the parameters involved. The notation $\Delta x_{\min}$ in the figures means the smallest grid-size in the problem. As was mentioned above the notation D.R.($C$) refers to the real part of the $s$-value located to the utmost right in the complex plane. The letter $C$ refers to the continuous problem while $D$ refers to the discrete problem. Ma is the

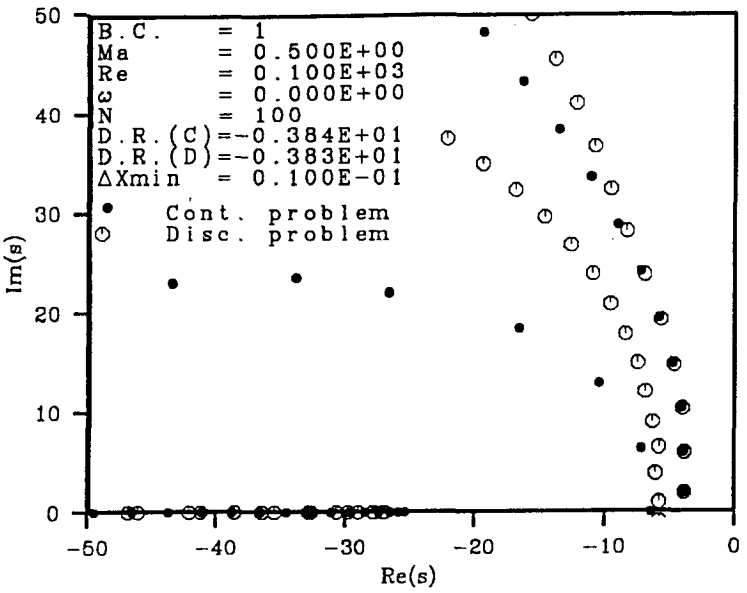


FIG. 2. Continuous and discrete spectrum for B.C.1, $\omega = 0$, uniform mesh.

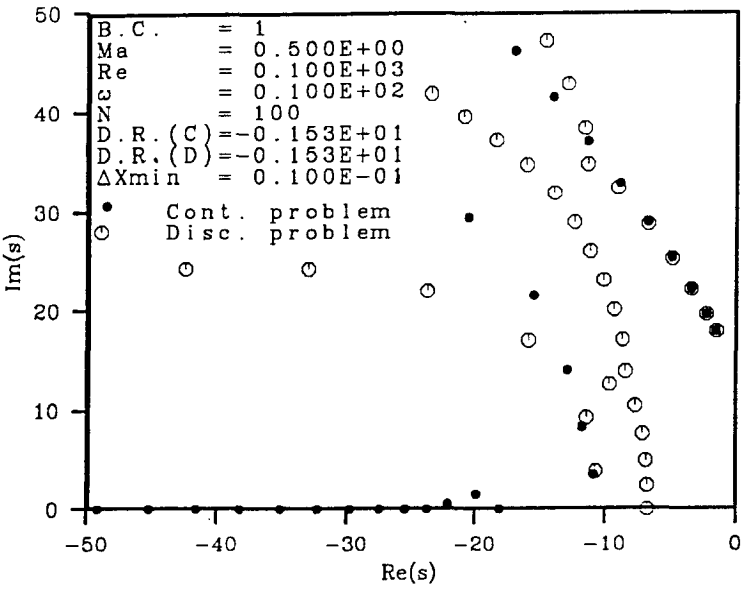


FIG. 3. Continuous and discrete spectrum for B.C.1, $\omega = 10$, uniform mesh.

Mach number and $\omega$ the wave number in the $y$ direction. A high value of $\omega$ corresponds to large $y$-derivatives and simulates the influence of gradients tangential to the boundaries.

We consider the continuous and discrete spectrum for B.C.1 when $\omega = 0$ and $\omega = 10$. As can be seen in Figs. 2 and 3 the agreement is excellent close to $s = 0$ in both cases. Note the accurate prediction of the decay rate. It is interesting to see the knee-like form of the spectrum close to zero. This kind of behavior of the spectrum for $\omega \neq 0$ was also found by Engquist and Gustafsson [6] when they studied the Euler equations. The decay rate is lower for the case $\omega = 10$ (compare with Fig. 1). As was mentioned above we should expect convergence of the discrete spectrum to the continuous one as $N$ increases. Several comparisons were done using $N = 40$, 60, 80, 100 and the convergence was verified. The same observation that was made for B.C.1 holds also for the other boundary conditions and therefore we conclude that the codes calculating the eigenvalues in the continuous and discrete cases are correct; this conclusion is supported by the 1-dimensional Navier–Stokes computations that are the topic of the next section.

## 6. Computations

By making computations using the full nonlinear Navier–Stokes equations we can check whether the predicted convergence rate (given by the linear analysis) agrees with the one obtained in practise. In order to compare with the analysis we tried to compute a uniform flow at Mach number 0.5 for different Reynolds numbers and meshes. The code used a centered finite-volume discretisation in space and the classical fourth-order Runge–Kutta method in time. It is a 2-dimensional code where symmetry conditions were applied in the $y$-direction. In all the computations 40 gridpoints were used with two different distributions, one uniform distribution and one distribution using formula (59),

$$\begin{aligned} x_i &= (1 + \cos(\Theta_i))/2 \\ \Theta_i &= \pi - i(\pi/N), \qquad i = 0, 1, \ldots, N. \end{aligned} \tag{59}$$

The transformation (59) (called a Tchebycheff mesh in the figures) clusters points close to the boundaries $x = 0$ and $x = 1$. This grid is not a natural choice for real computations since we are considering boundary conditions for open boundaries far from regions where physical gradients exist. From a mathematical point of view the Navier–Stokes equations admits a boundary layer type of eigensolution and it is therefore of interest to use a mesh with capability to resolve large gradients at the boundary.

As the initial condition in most of the computations a fraction (normally 10% of the maximum amplitude) of the real part of the least stable eigenvector was added to the freestream solution. The least stable eigenvector is the one corresponding to

the decay rate. By using the spectra one can compute a theoretical decay of the disturbance using the fourth-order Runge–Kutta amplification factor:

$$\|\phi(n\,\Delta t)\| = \|\phi(0)\| \times \left| \sum_{i=0}^{4} \frac{(s^*\,\Delta t)^i}{i!} \right|^n. \tag{60}$$

In (60) $s^*$ is the $s$ value with the real part equal to the decay rate and $n$ is the number of iterations. The solution should grow or decay with that rate. The use of (60) is indicated in the figures by a straight line. The time step $\Delta t$ is chosen to be constant and adjusted so that the CFL condition for the fourth-order Runge–Kutta method is satisfied:

$$\Delta t\,|s|_{\max} \leqslant \mathrm{CFL}_{(\cdot)}, \qquad \mathrm{CFL}_{(\mathrm{I})} = 2.828, \qquad \mathrm{CFL}_{(\mathrm{R})} = 2.875. \tag{61}$$

By $\mathrm{CFL}_{(\mathrm{I})}$ and $\mathrm{CFL}_{(\mathrm{R})}$ we denote the CFL numbers for a purely imaginary and purely real spectrum, respectively. Normally the time step was limited due to the elongation of the spectrum along the negative real axis, the time step was calculated using $\mathrm{CFL}_{(\mathrm{R})}$ and then reduced by approximately 30%. The reduction was made in order to avoid the eigenvalue located to the utmost left in the complex plane having the least damping. For each computation it was checked that the least damping was obtained using $s^*$.

In Fig. 4 we have the convergence history for a uniform mesh at $\mathrm{Re} = 10$. All the boundary conditions except *no*: 4 converge, which is in agreement with the information from the spectra where all eigenvalues are located in the left complex plane except for B.C.4 where $s = 0$ is included in the spectrum. In Fig. 5 we have the convergence history for $\mathrm{Re} = 100$ and a Tchebycheff mesh. B.C.1 converge according to theory after approximately 7000 iterations. B.C.2 has a decay rate close to zero which gives extremely slow convergence. As usual, B.C.4 does not converge. The spectrum corresponding to B.C.3 has eigenvalues in the right halfplane, see Fig. 6, which theoretically means that the solution should grow without bound. Another computation using a much lower initial disturbance was made, see Fig. 7. By comparing Figs. 5 and 7 one realises that nonlinear effects are the reason that B.C.3 does not grow without bound. The predicted growth rate is quite accurate. In Fig. 8 we have the convergence history for $\mathrm{Re} = 1000$ and a Tchebycheff mesh. The theoretical decay rate agrees well with the results of the computations for B.C.1 and B.C.3. For B.C.4 we have no convergence as usual and the convergence rate for B.C.2 is small, all in agreement with the theoretical analysis.

The results from the computations agree well with the theoretical analysis. They indicate that B.C.1 give fast convergence for all cases. B.C.2 converges always, but very slowly. B.C.3 give fast convergence if the mesh is coarse relative to the Reynolds number, and we have no convergence at all if the mesh is sufficiently fine. B.C.4 give no convergence at all due to the zero eigenvalue.

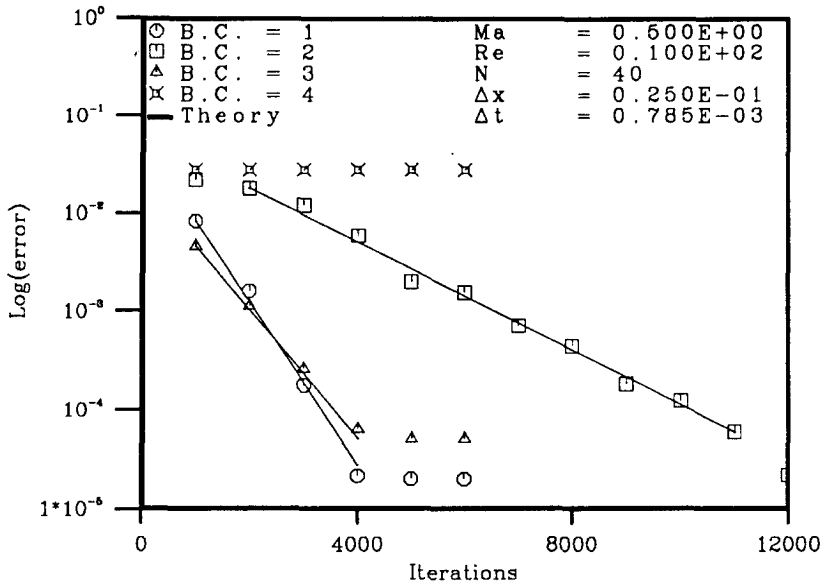


FIG. 4. Convergence history, Re = 10, uniform mesh.

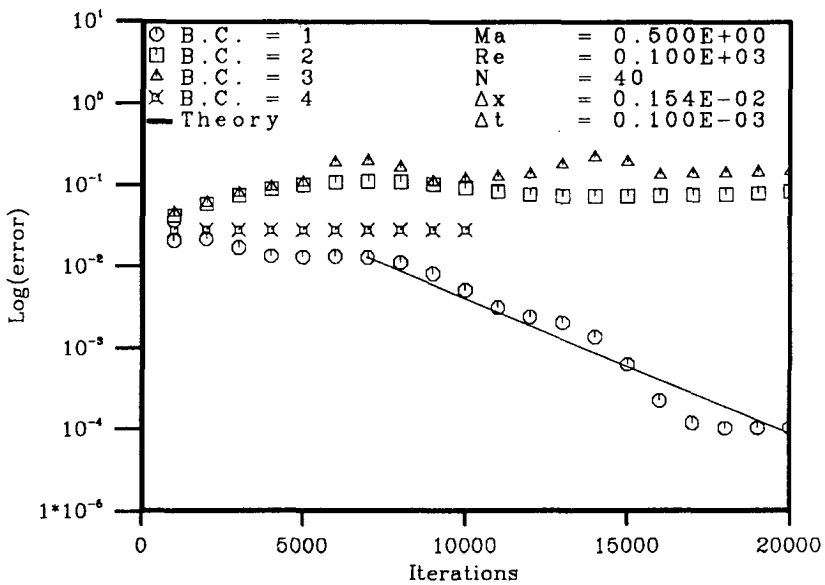


FIG. 5. Convergence history, Re = 100, Tcheb. mesh.

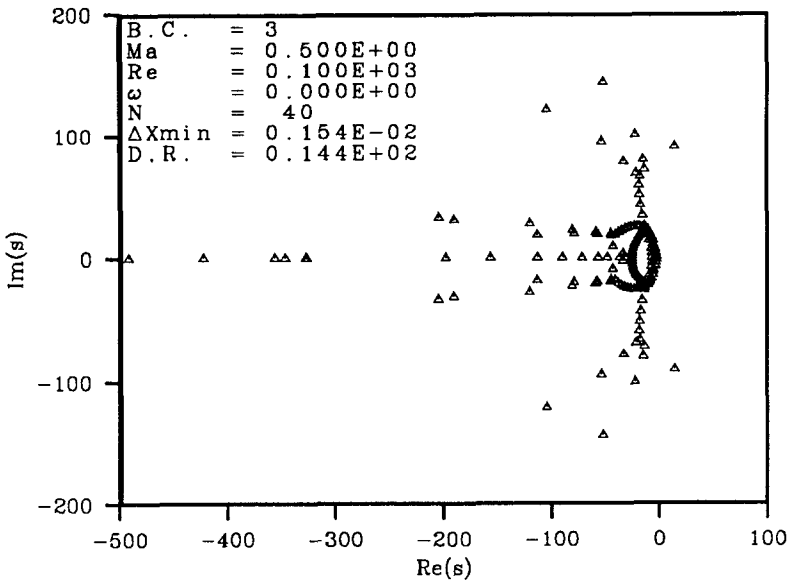


FIG. 6. The spectrum for B.C.3, view of origin, Re = 100, Tcheb. mesh.

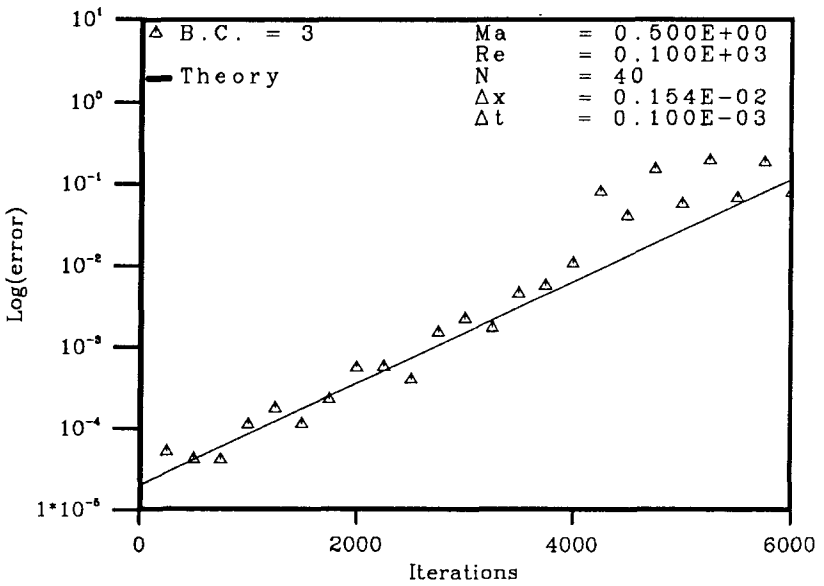


FIG. 7. The growth of a small disturbance for B.C.3, Re = 100, Tcheb. mesh.

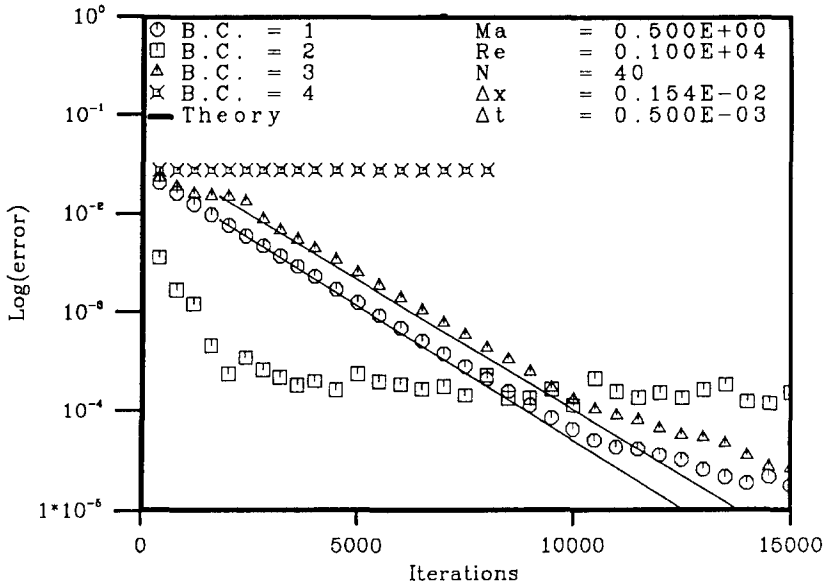


FIG. 8. Convergence history, Re = 1000, Tcheb. mesh.

## 7. NUMERICAL BOUNDARY CONDITIONS

As we have seen in the previous section the choice of numerical boundary conditions makes a great difference. By choosing to extrapolate $u$ instead of $\rho$ we did not get any convergence. The numerical calculations of the spectrum gave us the eigenvalue $s=0$. It is important not to use boundary conditions where $s=0$ is included in the spectrum for two reasons. First, as we have seen above, we do not get any convergence to steady state for the time-dependent problem. Second, consider the steady Navier–Stokes equations (corresponds to setting $s=0$ in (18)). If we apply boundary conditions so that the time-dependent problem has a spectrum including $s=0$ then the steady problem has nonunique solutions. This can be realised by setting the initial condition $f$ to zero, which means that $H$ in (41) is also zero. If $|E(0)|=0$ we get an arbitrary solution, since the coefficients $\sigma$ are not necessarily zero. The eigenvector corresponding to $s=0$ (see Fig. 9) has the form

$$\phi_i=(\rho_i, 0, 0, 0)^{\mathrm{T}}. \tag{62}$$

By setting $(\phi_i)_t=0$ in (45) and assuming the form (62) of the eigenvector, we obtain

$$\rho_i=\sigma_1+\sigma_2(-1)^i. \tag{63}$$

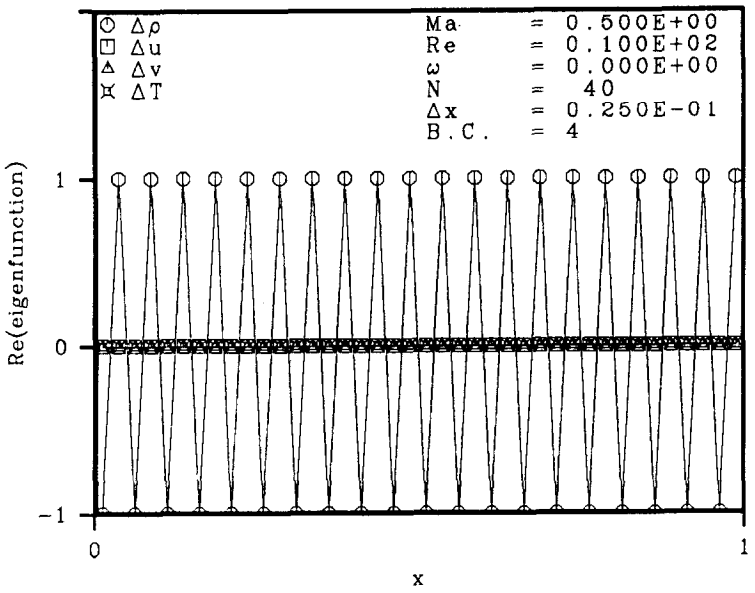


FIG. 9. The least stable eigenfunctions for B.C.4, Re = 10, uniform mesh.

The inflow and outflow conditions reduce to

$$\begin{aligned} \rho_0 + \rho_1 &= 0 \\ \rho_N + \rho_{N+1} &= 0. \end{aligned} \tag{64}$$

Thus the eigenvector corresponding to $s = 0$ involves an undetermined constant,

$$\phi_i = (\sigma_2(-1)^i, 0, 0, 0)^T. \tag{65}$$

Since all the other eigenvalues are located in the left half of the complex plane the corresponding eigenvectors should have disappeared after a sufficiently long time (sufficiently many iterations) and the whole error should be of the form (65). To investigate whether this was true or not for the full nonlinear problem another computation (Re = 10, uniform mesh) using a constant initial condition $f = 0.1 \times \tilde{q}$ was made. The error after 10,000 iterations for B.C.4 can be seen in Fig. 10. The error in $u$, $v$, and $T$ are small while the error in $\rho$ is several orders of magnitude larger and, furthermore, it has exactly the oscillating form (65) derived above.

If $\rho$ was extrapolated we obtained convergence for all the cases investigated. Furthermore, we have proved that the continuous boundary condition gives a well-posed problem. This encourages us to try and prove well-posedness also for the semi-discrete problem. We will restrict ourselves to the case with a uniform mesh, the extension to a nonuniform mesh is straightforward.

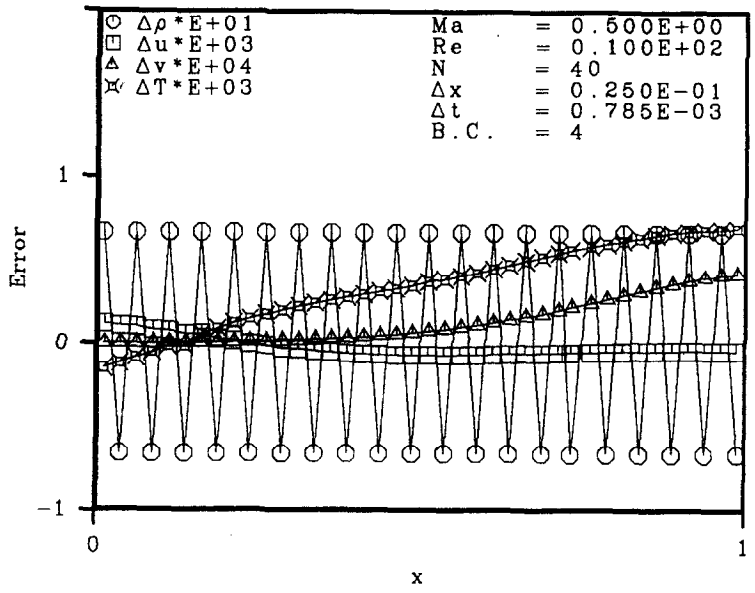


FIG. 10. The error after 10000 iterations for B.C.4, Re = 10, uniform mesh.

By using the finite volume method on a uniform mesh we get the semi-discrete correspondence to (14),

$$\begin{aligned} &(q_i)_t + AD_0 q_i + B(q_y)_i + \\ &\varepsilon\{CD_+ D_- q_i + ED_0(q_y)_i + D(q_{yy})_i\} = 0, \qquad i = 1, 2, ..., N, \quad t \geqslant 0 \\ &q_i(y, 0) = f_i(y), \qquad i = 0, 1, 2, ..., N+1 \\ &q_0 = B_0 q_1 + C_0 q_2 \\ &q_{N+1} = B_N q_N + C_N q_{N-1}, \end{aligned} \tag{66}$$

where $x_i = i\,\Delta x$ and $\Delta x = 1/N$. The forward, backward, and central difference operators are given by

$$D_+ q_i = (q_{i+1} - q_i)/\Delta x, \quad D_- q_i = (q_i - q_{i-1})/\Delta x, \quad D_0 q_i = (q_{i+1} - q_{i-1})/2\Delta x. \tag{67}$$

We will also use a special type of norm,

$$\begin{aligned} &\|\hat{q}\|_\delta^2 = \|\phi\|_\delta^2 = \phi_1^* \Lambda_1 \phi_1 \Delta x + \sum_{i=2}^{N-1} \phi_i^* \phi_i \Delta x + \phi_N^* \Lambda_N \phi_N \Delta x \\ &\|q\|_\delta^2 = \int_{-\infty}^{+\infty} \|\phi\|_\delta^2 \, d\omega = \int_{-\infty}^{+\infty} \left\{ q_1^{\mathrm{T}} \Lambda_1 q_1 \Delta x + \sum_{i=2}^{N-1} q_i^{\mathrm{T}} q_i \Delta x + q_N^{\mathrm{T}} \Lambda_N q_N \Delta x \right\} dy, \end{aligned} \tag{68}$$

where $\Lambda_1 = \mathrm{diag}(\delta_1, 1, 1, 1)$ and $\Lambda_N = \mathrm{diag}(\delta_N, 1, 1, 1)$. The parameters $\delta_1$ and $\delta_N$ are positive and will be specified later. Furthermore, we will need the two matrices $\chi^{(1)}$ and $\chi^{(N)}$ defined by

$$\begin{aligned}
\chi_{11}^{(1)} &= (1/2)\{B_0^{\mathrm{T}} A \Lambda_1 + \Lambda_1 A B_0\} \\
&\quad + (\varepsilon/\Delta x)\{-\theta B_0^{\mathrm{T}} C B_0 - (1-\theta)[B_0^{\mathrm{T}} C + C B_0] + (2(1-\theta)+1) C\} \\
\chi_{12}^{(1)} &= (1/2)\{\Lambda_1 A C_0 + (I - \Lambda_1) A\} \\
&\quad + (\varepsilon/\Delta x)\{-\theta B_0^{\mathrm{T}} C C_0 - (1-\theta)\, C(C_0 + I)\} \\
\chi_{21}^{(1)} &= (1/2)\{C_0^{\mathrm{T}} A \Lambda_1 + A(I - \Lambda_1)\} \\
&\quad + (\varepsilon/\Delta x)\{-\theta C_0^{\mathrm{T}} C B_0 - (1-\theta)(C_0 + I)^{\mathrm{T}} C\} \\
\chi_{22}^{(1)} &= (\varepsilon/\Delta x)\{-\theta C_0^{\mathrm{T}} C C_0 + (1-\theta) C\}
\end{aligned} \tag{69}$$

$$\begin{aligned}
\chi_{11}^{(N)} &= (1/2)\{B_N^{\mathrm{T}} A \Lambda_N + \Lambda_N A B_N\} \\
&\quad + (\varepsilon/\Delta x)\{+\theta B_N^{\mathrm{T}} C B_N + (1-\theta)[B_N^{\mathrm{T}} C + C B_N] - (2(1-\theta)+1) C\} \\
\chi_{12}^{(N)} &= (1/2)\{\Lambda_N A C_N + (I - \Lambda_N) A\} \\
&\quad + (\varepsilon/\Delta x)\{+\theta B_N^{\mathrm{T}} C C_N + (1-\theta)\, C(C_N + I)\} \\
\chi_{21}^{(N)} &= (1/2)\{C_N A \Lambda_N + A(I - \Lambda_N)\} \\
&\quad + (\varepsilon/\Delta x)\{+\theta C_N^{\mathrm{T}} C B_N + (1-\theta)(I + C_N)^{\mathrm{T}} C\} \\
\chi_{22}^{(N)} &= (\varepsilon/\Delta x)\{+\theta C_N^{\mathrm{T}} C C_N - (1-\theta) C\}.
\end{aligned} \tag{70}$$

The parameter $\theta$ in (69) and (70) satisfies

$$[(\bar{\lambda} + \bar{\mu})/(\bar{\lambda} + 2\bar{\mu})]^2/4 < \theta \leqslant 1. \tag{71}$$

We now state the result by which it will be shown that B.C.1 leads to a well-posed problem.

THEOREM 3. *If the matrices $B_0$, $C_0$, $B_N$, and $C_N$ in* (66) *are such that the conditions*

$$x^{\mathrm{T}} \begin{pmatrix} \chi_{11}^{(1)} & \chi_{12}^{(1)} \\ \chi_{21}^{(1)} & \chi_{22}^{(1)} \end{pmatrix} x \leqslant 0 \tag{72}$$

$$x^{\mathrm{T}} \begin{pmatrix} \chi_{11}^{(N)} & \chi_{12}^{(N)} \\ \chi_{21}^{(N)} & \chi_{22}^{(N)} \end{pmatrix} x \geqslant 0 \tag{73}$$

*are satisfied for all $x \neq 0$, then the problem is well posed and $q$ satisfies the estimate*

$$\|q\|_\delta^2 + \varepsilon\alpha \int_0^t \{\|q_y^{(2)}\|_\delta^2 + (1/2)(\|D_+ q^{(2)}\|_\delta^2 + \|D_- q^{(2)}\|_\delta^2)\}\, d\tau \leqslant \|f\|_\delta^2. \tag{74}$$

*We have used the notation* $q^{(2)} = (q_2, q_3, q_4)^T$ *and* $\alpha$ *is a positive constant of order one.*

*Proof.* By Fourier transforming (66) and using (68) we obtain

$$\begin{aligned}(\|\phi\|_\delta^2)_t = &+ (1/2)\{\phi_0^* A \Lambda_1 \phi_1 + \phi_1^* \Lambda_1 A \phi_0 + \phi_2^* A(I-\Lambda_1)\phi_1 + \phi_1^*(I-\Lambda_1) A\phi_2\} \\ &+ (\varepsilon/\Delta x)\{\phi_1^* C \phi_1 - \phi_0^* C \phi_0\} \\ &- (1/2)\{\phi_{N+1}^* A \Lambda_N \phi_N + \phi_N^* \Lambda_N A \phi_{N+1} + \phi_{N-1}^* A(I-\Lambda_N)\phi_N \\ &+ \phi_N^*(I-\Lambda_N) A \phi_{N-1}\} \\ &- (\varepsilon/\Delta x)\{\phi_{N+1}^* C \phi_{N+1} - \phi_N^* C \phi_N\} \\ &+ \varepsilon \sum_{i=1}^{N} Y_i^* \Psi Y_i \, \Delta x, \end{aligned} \tag{75}$$

where

$$Y_i^* \Psi Y_i = \begin{pmatrix} \phi_i i\omega \\ D_+ \phi_i \\ D_- \phi_i \end{pmatrix}^* \begin{pmatrix} 2D & E/2 & E/2 \\ E/2 & C & 0 \\ E/2 & 0 & C \end{pmatrix} \begin{pmatrix} \phi_i i\omega \\ D_+ \phi_i \\ D_- \phi_i \end{pmatrix}. \tag{76}$$

The matrix $\Psi$ is negative definite. It is easily verified also that the reduced matrix $\Psi_r$,

$$\Psi_r = \begin{pmatrix} 2D & E/2 & E/2 \\ E/2 & \theta C & 0 \\ E/2 & 0 & \theta C \end{pmatrix}, \tag{77}$$

is negative definite if $\theta$ is within the bounds given by (71). $\Psi_r$ is used in the sum instead of $\Psi$ for the points $i = 1$ and $i = N$. The remaining part of the matrix

$$\Psi_b = \Psi - \Psi_r = \begin{pmatrix} 0 & 0 & 0 \\ 0 & (1-\theta)C & 0 \\ 0 & 0 & (1-\theta)C \end{pmatrix} \tag{78}$$

is used to make the contribution from the boundary points more negative. Now we just have to make sure that the sum of the terms within the braces and the contribution from $\Psi_b$ have the right sign. By inserting the expression for the boundary points $\phi_0$ and $\phi_{N+1}$ into (75) we arrive at the equation:

$$\begin{aligned}(\|\phi\|_\delta^2)_t - \varepsilon Y_1^* \Psi_r Y_1 \, \Delta x - \varepsilon \sum_{i=2}^{N-1} Y_i^* \Psi Y_i \, \Delta x - \varepsilon Y_N^* \Psi_r Y_N \, \Delta x \\ = \begin{pmatrix} \phi_1 \\ \phi_2 \end{pmatrix}^* \chi^{(1)} \begin{pmatrix} \phi_1 \\ \phi_2 \end{pmatrix} - \begin{pmatrix} \phi_N \\ \phi_{N-1} \end{pmatrix}^* \chi^{(N)} \begin{pmatrix} \phi_N \\ \phi_{N-1} \end{pmatrix}. \end{aligned} \tag{79}$$

By using Parseval's theorem, conditions (72), (73), and (68) we obtain

$$(\|q\|_\delta^2)_t + \varepsilon\alpha\{\|q_y^{(2)}\|_\delta^2 + (1/2)(\|D_+ q^{(2)}\|_\delta^2 + \|D_- q^{(2)}\|_\delta^2)\} \leqslant 0. \tag{80}$$

The energy estimate (74) is obtained by integration. Uniqueness follows directly from (74) and, since existence is no problem (we are considering a linear system of ordinary differential equations where existence is known), we have proved the theorem.

Using the theorem above we will now investigate whether B.C.1 leads to a well-posed problem. We begin by studying the outflow terms. The matrices $B_N$ and $C_N$ are given by discretising the outflow conditions in (56) and using linear extrapolation of $\rho$,

$$B_N = \begin{pmatrix} 2 & 0 & 0 & 0 \\ \left(\frac{3}{2}\right)\left(\frac{\Delta x}{\varepsilon}\right)\left(\frac{\bar{c}}{\sqrt{\gamma}}\right)\frac{\bar{\rho}}{(\bar{\lambda}+2\bar{\mu})} & 1 & 0 & \left(\frac{\Delta x}{\varepsilon}\right)\left(\sqrt{\frac{(\gamma-1)}{\gamma}}\,\bar{c}\right)\frac{\bar{\rho}}{(\bar{\lambda}+2\bar{\mu})} \\ 0 & 0 & 1 & 0 \\ 0 & 0 & 0 & 1 \end{pmatrix} \tag{81}$$

$$C_N = \begin{pmatrix} -1 & 0 & 0 & 0 \\ -\left(\frac{1}{2}\right)\left(\frac{\Delta x}{\varepsilon}\right)\left(\frac{\bar{c}}{\sqrt{\gamma}}\right)\frac{\bar{\rho}}{(\lambda+2\bar{\mu})} & 0 & 0 & 0 \\ 0 & 0 & 0 & 0 \\ 0 & 0 & 0 & 0 \end{pmatrix}. \tag{82}$$

The matrix $\chi^{(N)}$ can be separated into parts of different orders of magnitude,

$$\chi^{(N)} = \chi^{(N)}_{O(\varepsilon/\Delta x)} + \chi^{(N)}_{O(1)} + \chi^{(N)}_{O(\Delta x/\varepsilon)}. \tag{83}$$

Simple but tedious algebra gives

$$\begin{aligned} x^{\mathrm{T}}\chi^{(N)}_{O(\varepsilon/\Delta x)}x = \bar{\rho}^{-1}(\varepsilon/\Delta x)(1-\theta)\{&(\bar{\lambda}+2\bar{\mu})(x_2-x_6)^2 \\ &+ \bar{\mu}(x_3-x_7)^2 + (\gamma\bar{k}/\mathrm{Pr})(x_4-x_8)^2\}. \end{aligned} \tag{84}$$

Obviously the quadratic form (84) is non-negative. We continue with the terms of order one,

$$\begin{aligned} x^{\mathrm{T}}\chi^{(N)}_{O(1)}x = \bar{u}\{&2\delta_N x_1^2 + x_2^2 + x_3^2 + x_4^2 + (1-2\delta_N)\,x_1x_5\} \\ &+ (\bar{c}/\sqrt{\gamma})(\delta_N - 1)\,x_1(x_2 - x_6). \end{aligned} \tag{85}$$

We will now make use of $\delta_N$ to remove the mixed involving $x_5$, this is accomplished by choosing $\delta_N = \frac{1}{2}$. Having made that choice we obtain

$$x^T\chi^{(N)}x = \tilde{\rho}^{-1}(\varepsilon/\Delta x)(1-\theta)\{(\bar{\lambda}+2\bar{\mu})(x_2-x_6)^2 + \bar{\mu}(x_3-x_7)^2 + (\gamma\bar{k}/\mathrm{Pr})(x_4-x_8)^2\} + \tilde{u}\{x_1^2+x_2^2+x_3^2+x_4^2\} - (1/2)(\bar{c}/\sqrt{\gamma})\,x_1(x_2-x_6) + O(\Delta x/\varepsilon). \quad (86)$$

By making use of the formula

$$2xy = (x\sqrt{\eta} + y/\sqrt{\eta})^2 - \eta x^2 - y^2/\eta \quad (87)$$

and letting $\Delta x \to 0$ we can use the large positive coefficient in front of $(x_2-x_6)^2$ to make the quadratic form (86) positive. Thus we have showed that the outflow terms have the right sign.

By using the same technique, one can easily show that also the inflow terms have the right sign (the algebra is less complicated since only two boundary points are involved). The matrix $C_0$ is identically zero and we can choose $\delta_1 = 1$. The matrix $B_0$ is found by discretising the inflow boundary conditions in (56) and is given below for reference:

$$B_0 = \begin{pmatrix} -1 & (\zeta-1)/\sqrt{\gamma} & 0 & (\zeta+1)/\sqrt{\gamma-1} \\ 0 & -\zeta & 0 & -\sqrt{\gamma/(\gamma-1)}(\zeta+1) \\ 0 & 0 & -1 & 0 \\ 0 & \sqrt{(\gamma-1)/\gamma}(\zeta-1) & 0 & \zeta \end{pmatrix} \quad (88)$$

$$\zeta = \{(\gamma-1)(\gamma\bar{k}/\mathrm{Pr}) - \gamma(\bar{\lambda}+2\bar{\mu})\}/\{(\gamma-1)(\gamma\bar{k}/\mathrm{Pr}) + \gamma(\bar{\lambda}+2\bar{\mu})\}. \quad (89)$$

We can summarise the result in a theorem.

THEOREM 4. *If the matrices* $B_0$, $B_N$, *and* $C_N$ *given by* (88)), (81), *and* (82) *respectively are used in the boundary conditions then problem* (66) *is well posed and the solution satisfies the estimate* (74).

We conclude this section with some remarks concerning B.C.4. If we apply Theorem 3 to B.C.4 we find that the condition (72) is satisfied (we have the same inflow conditions as for B.C.1) while the condition (73) is violated. By assuming the form (65) of $\phi$ we get from (79) that $(\|\phi\|_\delta^2)_t = 0$ as one would expect from the previous analysis.

## 8. TIME INTEGRATION

Finally, we shall discuss some implications of the results obtained so far concerning the numerical time integration of the Navier–Stokes equations. Traditionally the influence of boundary conditions on choosing the time-integration method has been

ignored. A simplified analysis based on the assumption that the problem is periodic (or has an infinite domain) and thus allows one to Fourier-transform the spatial part has been used. The spectra obtained in this way is then the basis when the time-integration method is chosen. As will be shown below, this type of analysis might predict the wrong location or shape of the spectrum and one might therefore choose the wrong time-integration method.

We need the well-known concept of absolute stability.

DEFINITION 3. The region of absolute stability of a numerical method for an initial value problem is that set of complex values of $s\,\Delta t$ for which all approximations $u^n = u(n\,\Delta t)$ applied to the test problem

$$u_t = su, \qquad u(0) = 1 \tag{90}$$

will remain bounded as $n \to \infty$.

We will proceed as follows: first we choose a suitable time-integration method where the spectrum for periodic boundary conditions (hereafter denoted by B.C.P.) is included in the region of absolute stability. Next we investigate if that time-integration method applied to the problem with B.C.1 or B.C.3 leads to a stable computation. One case with high spatial resolution (Re = 10, Tchebycheff mesh) and one with low spatial resolution (Re = 100, uniform mesh) will be considered.

In Figs. 11 and 12 we see the spectrum for B.C.P. in the high resolution case. Since the spectrum stretches far out along the negative real axis we need a method

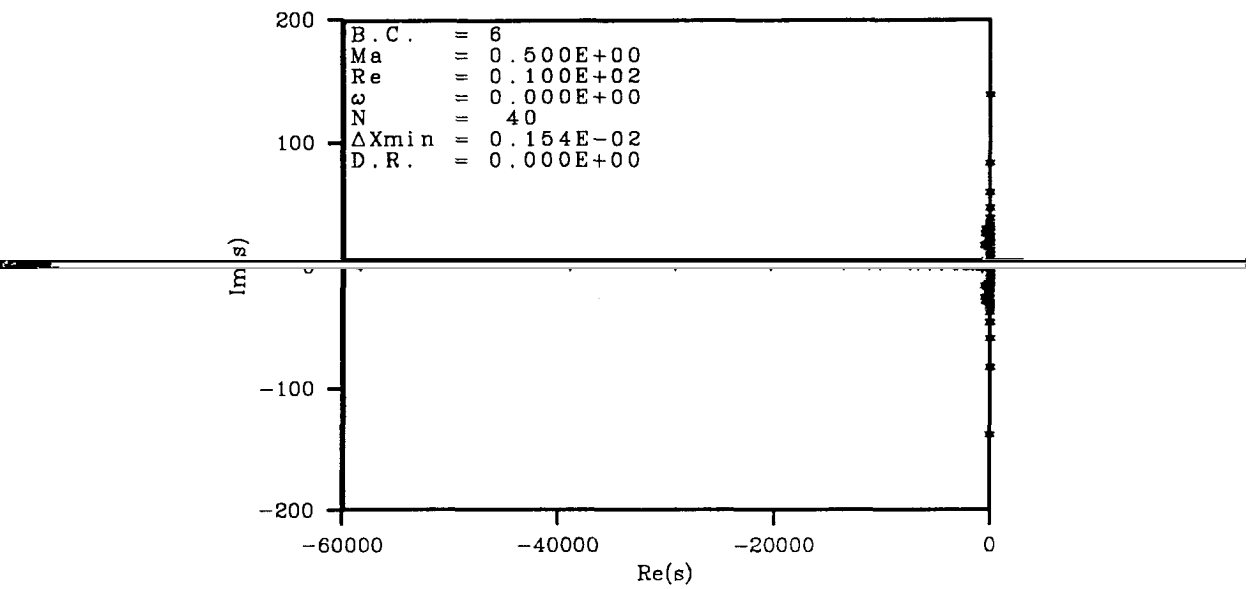


FIG. 11. The spectrum for B.C.P., global view, Re = 10, Tcheb. mesh.

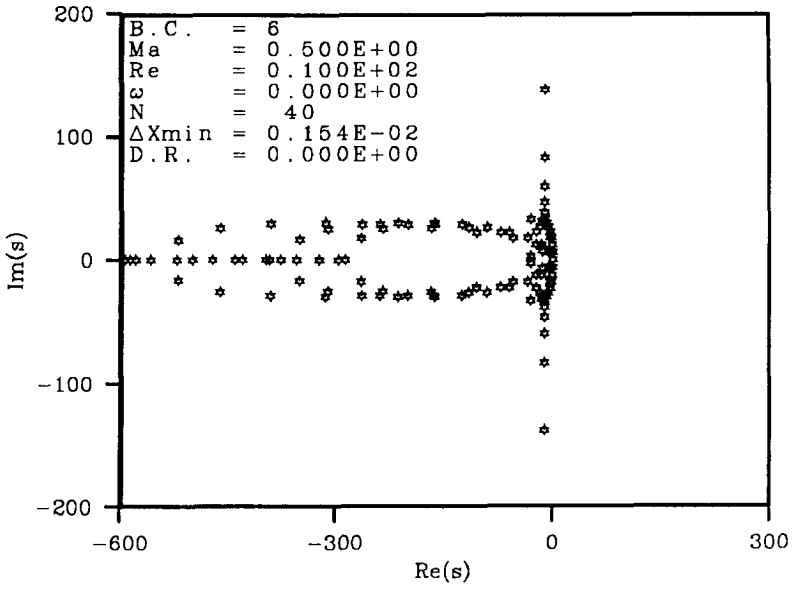


FIG. 12. The spectrum for B.C.P., view of origin, Re = 10, Tcheb. mesh.

with a large region of absolute stability in the left half of the complex plane. This suggests some type of implicit method. As an example we might choose the trapezoidal method which applied to (90) gives us

$$u^n = [(1 + s\,\Delta t/2)/(1 - s\,\Delta t/2)]^n. \tag{91}$$

The trapezoidal method is absolutely stable for all $\Delta t$ if $\Re(s) \leqslant 0$. The spectra given by B.C.1 and B.C.3 are shown in Figs. 13–16. Since the whole spectrum for B.C.1 is located in the region of absolute stability, $u^n$ will be bounded for all $n$. The spectrum for B.C.3 has eigenvalues far out in the right half of the complex plane (outside the region of absolute stability) and $u^n$ will become unbounded as $n \to \infty$.

In the low resolution case we have the spectrum for B.C.P. in Fig. 17. The shape and location of the spectrum suggests that an explicit method might be suitable. As an example we might choose the classical fourth-order Runge–Kutta method which applied to (90) give us the solution

$$u^n = [1 + (s\,\Delta t) + (s\,\Delta t)^2/2! + (s\,\Delta t)^3/3! + (s\,\Delta t)^4/4!]^n. \tag{92}$$

By using formula (61), where $|s|_{\max} \simeq 125$ is found in Fig. 17, we obtain a suitable time-step $\Delta t_{\text{B.C.P.}} = 0.021 \simeq \text{CFL}_{(\text{R})}/|s|_{\max}$ leading to a stable method for B.C.P. The solid lines in Figs. 17–19 show the expanded (multiplied with $\Delta t_{\text{B.C.P}}^{-1}$) region of absolute stability for the fourth-order Runge–Kutta method. Since the whole spectrum for B.C.3 (shown in Fig. 19) is located inside the expanded region of absolute stability, $u^n$ will be bounded for all $n$. The spectrum for B.C.1 (shown in

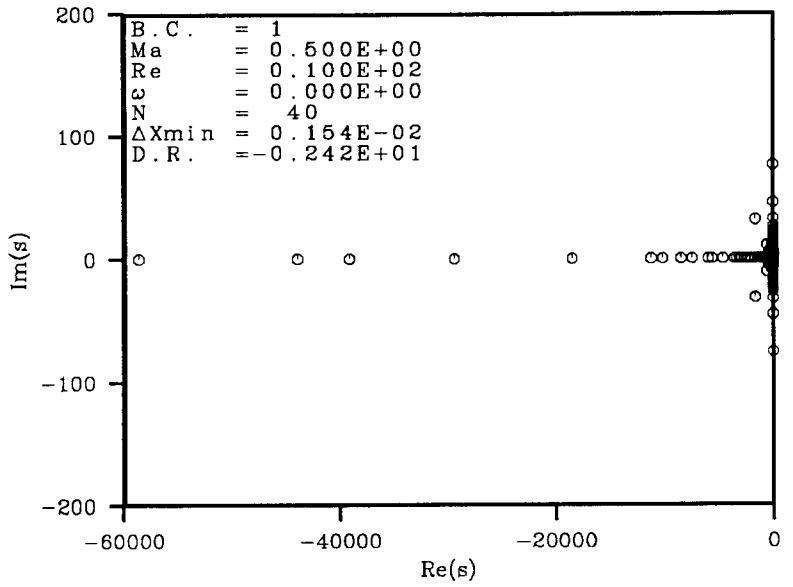


FIG. 13. The spectrum for B.C.1, global view, Re = 10, Tcheb. mesh.

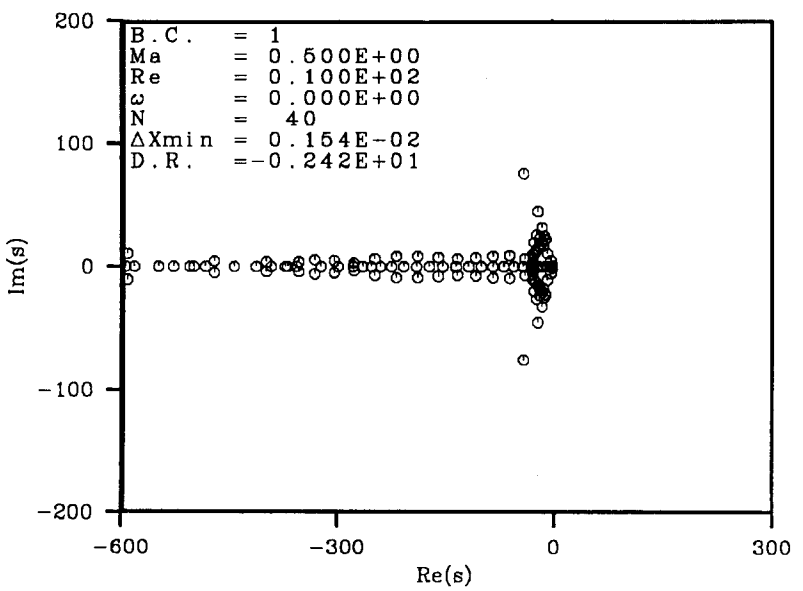


FIG. 14. The spectrum for B.C.1, view of origin, Re = 10, Tcheb. mesh.

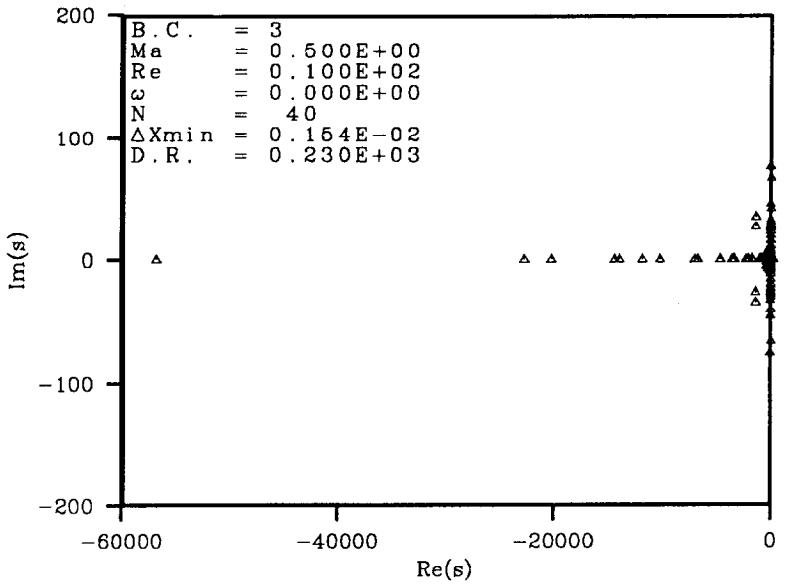


FIG. 15. The spectrum for B.C.3, global view, Re = 10, Tcheb. mesh.

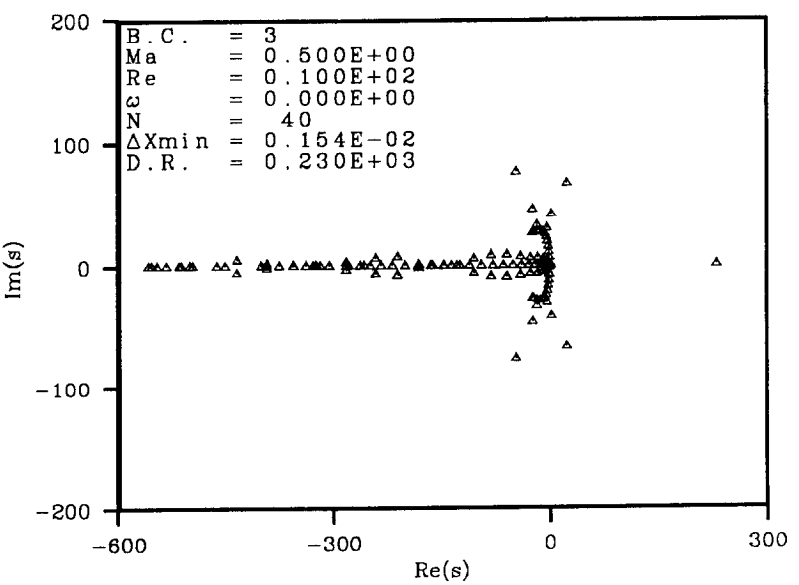


FIG. 16. The spectrum for B.C.3, view of origin, Re = 10, Tcheb. mesh.

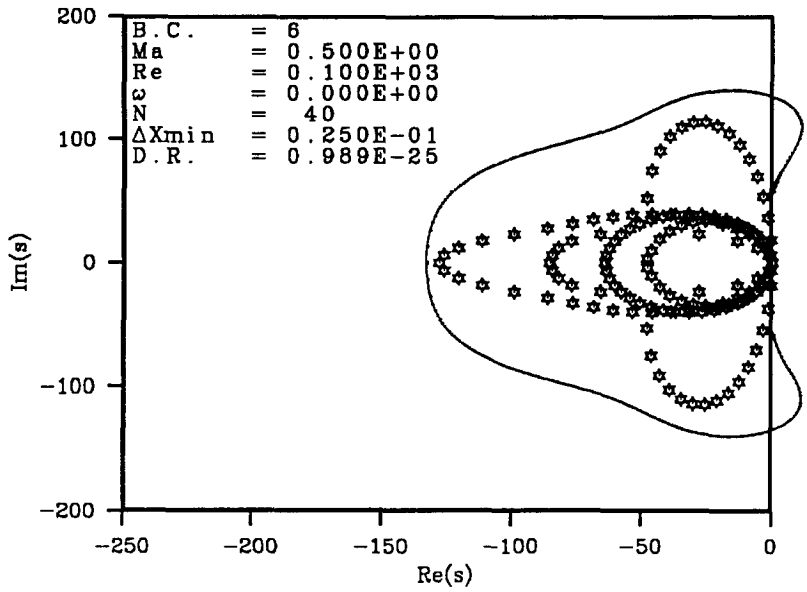


FIG. 17. The spectrum for B.C.P., Re = 100, uniform mesh.

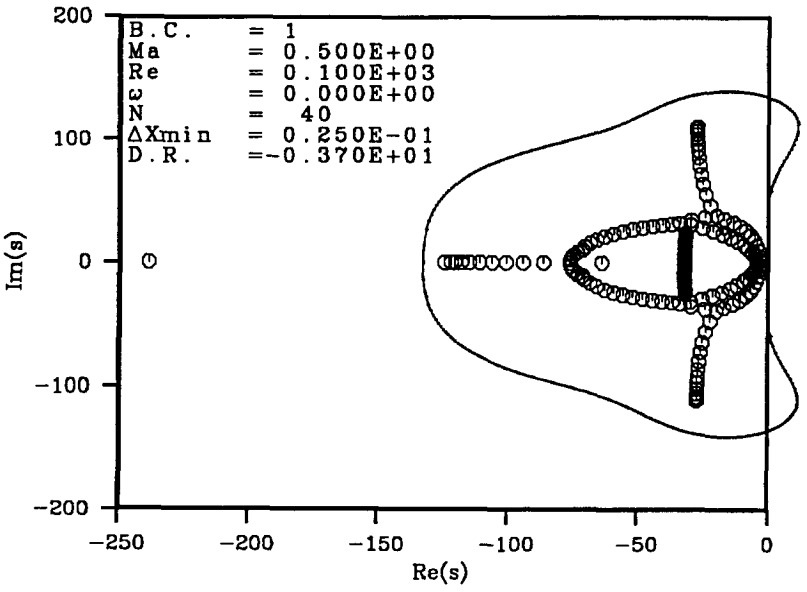


FIG. 18. The spectrum for B.C.1, Re = 100, uniform mesh.

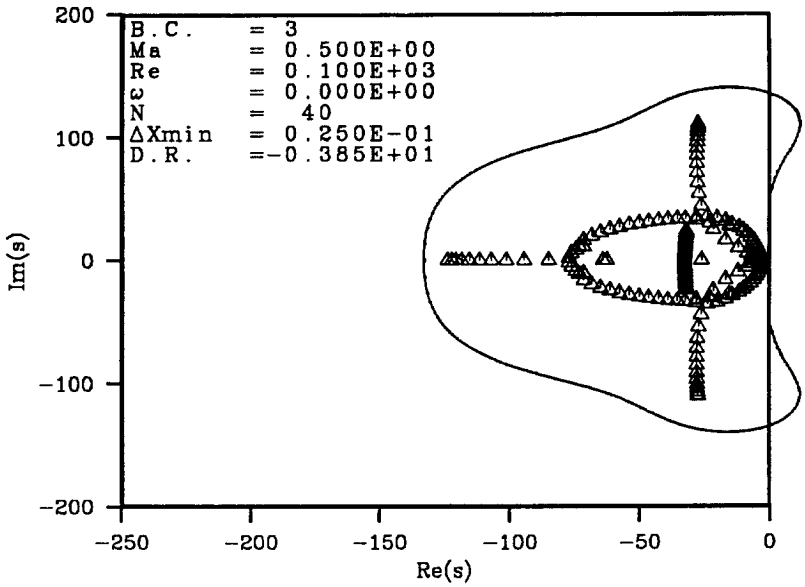


FIG. 19. The spectrum for B.C.3, Re = 100, uniform mesh.

Fig. 18) has a single eigenvalue at $s \simeq -240$ which was not predicted by using B.C.P. That eigenvalue is located outside the expanded region of absolute stability and $u^n$ will become unbounded as $n \to \infty$.

## 9. CONCLUSIONS

The question of open boundary conditions for the Navier–Stokes equations has been addressed. Using the energy-method conditions for well-posedness of both the continuous and semi-discrete constant coefficient problem has been derived. The conditions derived by the energy method have been used to derive well posed boundary conditions of a dissipative type for the continuous problem and to show that well-posedness is preserved for the semi-discrete problem if a correct numerical boundary condition is used.

By using the Laplace transform technique a method to compute the influence of boundary conditions on the spectrum of both the continuous and semi-discrete problem has been derived. Using this method it has been shown how one can predict the rate of convergence to steady state. The method has been used to compare boundary conditions derived using the energy method and a couple of common boundary conditions used in the numerical calculations of the Navier–Stokes equations. The results indicate that the boundary conditions derived by the energy method are superior (give faster convergence to steady state) provided that the correct numerical boundary condition is used. It is also shown that the method of

using characteristic boundary conditions (with the numerical boundary conditions used here) is an unstable method if a sufficiently fine non-uniform mesh is used. The theoretical conclusions drawn by investigating the different spectra are confirmed by the 1-dimensional Navier–Stokes computations.

The problem with choosing the right numerical boundary condition has been addressed. The well-posed continuous boundary conditions are discretised and two different types of numerical boundary conditions are investigated. By extrapolating the normal velocity we obtained a scheme with zero convergence rate for the time-dependent problem and non-unique solutions of the stationary problem. On the other hand, by extrapolating the density we are able to prove that the semi-discrete problem is well posed.

Finally some comparisons with spectra obtained assuming periodic boundary conditions and spectra including the effect of boundary conditions were made. It was shown that the assumption of periodic boundary conditions might give the wrong spectrum and as a consequence one might choose the wrong time-integration method.

## Appendix

$$A = \begin{pmatrix} \bar{u} & \bar{c}/\sqrt{\gamma} & 0 & 0 \\ \bar{c}/\sqrt{\gamma} & \bar{u} & 0 & \sqrt{\frac{(\gamma-1)}{\gamma}}\,\bar{c} \\ 0 & 0 & \bar{u} & 0 \\ 0 & \sqrt{\frac{(\gamma-1)}{\gamma}}\,\bar{c} & 0 & \bar{u} \end{pmatrix} \tag{93}$$

$$B = \begin{pmatrix} \bar{v} & 0 & \bar{c}/\sqrt{\gamma} & 0 \\ 0 & \bar{v} & 0 & 0 \\ \bar{c}/\sqrt{\gamma} & 0 & \bar{v} & \sqrt{\frac{(\gamma-1)}{\gamma}}\,\bar{c} \\ 0 & 0 & \sqrt{\frac{(\gamma-1)}{\gamma}}\,\bar{c} & \bar{v} \end{pmatrix} \tag{94}$$

$$C = \begin{pmatrix} 0 & 0 & 0 & 0 \\ 0 & -(\bar{\lambda}+2\bar{\mu})/\bar{\rho} & 0 & 0 \\ 0 & 0 & -\bar{\mu}/\bar{\rho} & 0 \\ 0 & 0 & 0 & -(\gamma\bar{k}/\mathrm{Pr})/\bar{\rho} \end{pmatrix} \tag{95}$$

$$D = \begin{pmatrix} 0 & 0 & 0 & 0 \\ 0 & -\mu/\bar{\rho} & 0 & 0 \\ 0 & 0 & -(\bar{\lambda}+2\bar{\mu})/\bar{\rho} & 0 \\ 0 & 0 & 0 & -(\gamma\bar{k}/\mathrm{Pr})/\bar{\rho} \end{pmatrix} \tag{96}$$

$$E = \begin{pmatrix} 0 & 0 & 0 & 0 \\ 0 & 0 & -(\bar{\lambda}+\bar{\mu})/\bar{\rho} & 0 \\ 0 & -(\bar{\lambda}+\bar{\mu})/\bar{\rho} & 0 & 0 \\ 0 & 0 & 0 & 0 \end{pmatrix}. \tag{97}$$

## ACKNOWLEDGMENTS

I would like to thank NASA Ames for the large amount of computer time provided and Professor Bertil Gustafsson at Uppsala University for many fruitful and encouraging discussions.

## REFERENCES

1. D. H. RUDY AND J. C. STRIKWERDA, *Comput. & Fluids* **10** (1981).
2. B. GUSTAFSSON AND A. SUNDSTRÖM, *SIAM J. Appl. Math.* **35** (1978).
3. J. OLIGER AND A. SUNDSTRÖM, *SIAM J. Appl. Math.* **35** (1978).
4. J. NORDSTRÖM, in *Lecture Notes in Physics*, Vol. 264 (Springer-Verlag, Berlin/Heidelberg, 1986), p. 505.
5. P. DUTT, ICASE Report No. 85-37, 1985 (unpublished).
6. B. ENGQUIST AND B. GUSTAFSSON, *Math. Comput.* **49** (1987).
7. H. O. KREISS, *Commun. Pure Appl. Math.* **23** (1970).
8. H. O. KREISS AND J. LORENZ, Evolutionary systems and the Navier–Stokes equations (unpublished).
9. S. ABARBANEL AND D. GOTTLIEB, *J. Comput. Phys.* **35** (1981).
10. J. NORDSTRÖM, FFA TN 1985-08, 1985 (unpublished).
11. J. STRIKWERDA, *Commun. Pure Appl. Math.* **30** (1977).